MyD88-dependent, superoxide-initiated inflammation is necessary for flow-mediated inward remodeling of conduit arteries

Paul C.Y. Tang,[1] Lingfeng Qin,[1] Jacek Zielonka,[6] Jing Zhou,[1] Catherine Matte-Martone,[2] Sonia Bergaya,[3] Nico van Rooijen,[7] Warren D. Shlomchik,[2] Wang Min,[4] William C. Sessa,[3] Jordan S. Pober,[5] and George Tellides[1]

[1]Departments of Surgery, [2]Medical Oncology, [3]Pharmacology, [4]Pathology, and [5]Immunobiology, Interdepartmental Program in Vascular Biology and Therapeutics, Yale University School of Medicine, New Haven, CT 06510
[6]Department of Biophysics and Free Radical Research Center, Medical College of Wisconsin, Milwaukee, WI 53226
[7]Department of Molecular Cell Biology, Vrije Universiteit Medical Center, 1081 HV Amsterdam, Netherlands

Vascular remodeling normalizes abnormal hemodynamic stresses through structural changes affecting vessel size and wall thickness. We investigated the role of inflammation in flow-mediated vascular remodeling using a murine model of partial outflow reduction without flow cessation or neointima formation. Common carotid arteries decreased in size after ipsilateral external carotid artery ligation in wild-type mice, but not in myeloid differentiation protein-88 (MyD88)–deficient mice. Inward remodeling was associated with MyD88-dependent and superoxide-initiated cytokine and chemokine production, as well as transient adventitial macrophage accumulation and activation. Macrophage depletion prevented flow-mediated inward vascular remodeling. Expression of MyD88 by intrinsic vascular cells was necessary for cytokine and chemokine production and changes in vessel size, whereas MyD88 expression by bone marrow–derived cells was obligatory for changes in vessel size. We conclude that there are at least two distinct roles for MyD88 in flow-mediated inward remodeling of conduit arteries. Our findings suggest that inflammation is necessary for vascular adaptation to changes in hemodynamic forces.

CORRESPONDENCE
George Tellides:
george.tellides@yale.edu

Abbreviations used: α-SMA, α-smooth muscle actin; Cav, caveolin; DHE, dihydroethidium; EC, endothelial cell; EEL, external elastic lamina; ICE, IL-1β converting enzyme; IP-10, IFN-γ–induced protein of 10 kD; Mig, monokine induced by γ-IFN; MyD88, myeloid differentiation protein-88; NOS, nitric oxide synthase; q, quantitative; ROS, reactive oxygen species; SMC, smooth muscle cell; SOD, superoxide dismutase; TLR, Toll-like receptor; TRIF, TIR domain-containing adapter inducing IFN-β; TXN, thioredoxin; VCAM, vascular cell adhesion molecule.

The regulation of blood vessel size is closely coordinated to changes in blood flow. Initial variations in blood flow elicit reversible vasomotor responses, whereas sustained alterations in hemodynamic forces result in permanent structural changes affecting vessel external diameter and/or vessel wall thickness that are described as vascular remodeling (1, 2). These adaptive changes in vessel size and medial thickness serve to normalize abnormal vascular stresses initiated by developmental or physiological perturbations of hemodynamic forces. For example, increases in blood flow and shear stress after construction of an arteriovenous fistula induce outward remodeling, whereas decreases in blood flow and shear stress caused by ligation of arterial branches result in inward remodeling (3, 4). Vascular remodeling is integral to the development of the vasculature and the progression of arterial disease. Attenuated flow in the embryo leads to defective vascular growth that compromises viability (5), and inward remodeling of arteries distal to flow-limiting occlusive lesions results in luminal loss that further exacerbates tissue ischemia (6, 7).

The endothelium is responsible for the detection of shear stress and plays an essential role in flow-mediated vascular remodeling (8). Physical perturbation of various "mechanoreceptors" trigger a network of intracellular signaling pathways, collectively termed mechanotransduction, which activate several transcription factors, notably NF-κB, that regulate the expression of mechanosensitive genes and ultimately lead to vessel wall remodeling through cellular and extracellular matrix reorganization (9). The generation of reactive oxygen species

The Rockefeller University Press $30.00
J. Exp. Med. Vol. 205 No. 13 3159-3171
www.jem.org/cgi/doi/10.1084/jem.20081298

The Journal of Experimental Medicine

(ROS), including superoxide, hydrogen peroxide, and peroxynitrite, plays a central role in mechanotransduction (10). The predominant sources of superoxide in vascular cells are NADPH oxidases (11), whereas less significant amounts of superoxide are produced by nitric oxide synthase (NOS), xanthine oxidase, cytochrome P450, and cyclooxygenase activity (10). An additional major source of superoxide is the mitochondrial electron transport chain (12), and cross talk between mitochondrial ROS and NADPH oxidases has been described (13). Besides endogenous vascular cell production of superoxide, infiltrating macrophages within the arterial wall may also represent a source of ROS which can diffuse into the extracellular matrix and activate matrix metalloproteinases that are essential for vascular remodeling (14). Superoxide anion may directly signal or may be converted to other ROS; the presence of superoxide dismutase (SOD) leads to conversion to hydrogen peroxide or combination with nitric oxide forms peroxynitrite. These ROS may act as second messengers and modulate mechanotransduction signaling and gene transcription. Indeed, NADPH oxidases are required for outward vascular remodeling (15), and mitochondrial ROS is necessary for flow-mediated vasodilation (16).

In addition to direct effects on vascular tissues, ROS may promote recruitment of inflammatory leukocytes. For example, alterations in shear stress can lead to ROS-dependent NF-κB activation in endothelial cells (ECs) (17, 18). The activation of NF-κB, in turn, contributes to production of chemokines and cytokines by vascular cells that lead to the recruitment and activation of leukocytes within the artery wall. Vascular inflammation caused by microbial infection is also ROS dependent (19, 20). Endogenous vascular-derived factors, such as IL-1 (21), and exogenous pathogen-derived molecules are recognized by cells via surface IL-1Rs and Toll-like receptors (TLRs), respectively. Both the IL-1R (as well as the IL-18R) and most TLRs share a common signaling adaptor, myeloid differentiation protein-88 (MyD88), which induces activation of NF-κB through intermediary kinases and production of inflammatory cytokines and chemokines (22). The exceptions are TLR3, which signals exclusively through TIR domain–containing adaptor-inducing IFN-β (TRIF), and TLR4, which signals through both MyD88 and TRIF (23). MyD88 may also influence other cytokine responses, e.g., by contributing to the stability of certain mRNAs encoding proinflammatory proteins (24).

The accumulation of activated leukocytes within the intima is recognized as a key pathogenetic process in atherosclerosis (25). Infiltrating monocytes differentiate into macrophages that promote plaque progression and remodeling by sustaining inflammation, oxidative stress, and matrix turnover. In contrast to atherosclerotic changes, flow-mediated remodeling of conduit arteries in the absence of disease is not thought to be dependent on inflammatory responses. Suggestive evidence to the contrary is that TLR4 is necessary for outward remodeling of murine common carotid arteries after complete ligation of the contralateral vessel (26). Nonetheless, inflammation is not reported in this context, and TLR4 is not required for inward remodeling of common carotid arteries after ligation of the ipsilateral external and internal carotid arteries (2, 27). Interestingly, endothelial expression of proinflammatory molecules and leukocytic infiltrates have been noted in rabbit and mouse models with marked flow reduction in the common carotid artery caused by prevention of outflow from both internal and external carotid arteries (28–31). However, neointima also develops in these very low-flow models in rodents, and it is difficult to distinguish physiological adaptations from pathological remodeling. Similar caveats apply to complete arterial ligation models with an absence of blood flow (32–34), in which coagulation and platelet activation may further confound the interpretation of mechanisms for vascular remodeling in response to hemodynamic forces.

Here, we show that vascular inflammatory responses and macrophage function requiring MyD88 are necessary for flow-mediated, superoxide-dependent inward remodeling of common carotid arteries after partial outflow obstruction using an established murine model with proportional vessel shrinkage, but without flow cessation or neointima formation. Our new observations suggest that inflammatory responses may be central to vascular remodeling even in the absence of overt injury.

RESULTS

MyD88 is necessary for flow-mediated inward vascular remodeling

Because MyD88 is central to many innate immune responses, we first compared adaptive vascular remodeling in response to reduced blood flow in WT versus MyD88-deficient ($MyD88^{-/-}$) mice by measuring common carotid artery size and wall thickness after ipsilateral external carotid artery ligation (Fig. 1 a). Surgical occlusion of the branch vessel resulted in sustained 40–50% reduction in blood flow within the parent vessel in both strains (Fig. 1 b). As previously reported for WT mice (35), the left common carotid artery decreased 10–15% in external diameter without changes in medial thickness compared with the unmanipulated right vessel after 2 wk (Fig. 1, c and d). The remodeling changes occurred primarily between 3 and 7 d after the operation (Fig. S1 a, available at http://www.jem.org/cgi/content/full/jem.20081298/DC1). Strikingly, common carotid arteries in $MyD88^{-/-}$ mice did not inwardly remodel, but responded instead by medial thickening at 2 wk (Fig. 1, c and d). Vascular compartment areas derived from perimeter measurements showed similar results (though with enhanced differences caused by the second power relationship), except for medial atrophy in WT mice versus medial hypertrophy in $MyD88^{-/-}$ mice (Fig. S1, b and c).

Medial remodeling in response to flow reduction was primarily cellular (Table I and Fig. S2, available at http://www.jem.org/cgi/content/full/jem.20081298/DC1). Medial smooth muscle cells (SMCs) were lost largely from the outer lamella of left common carotid arteries in WT mice, such that two rather than three medial lamellar units were apparent for much of the vessel circumference. The medial

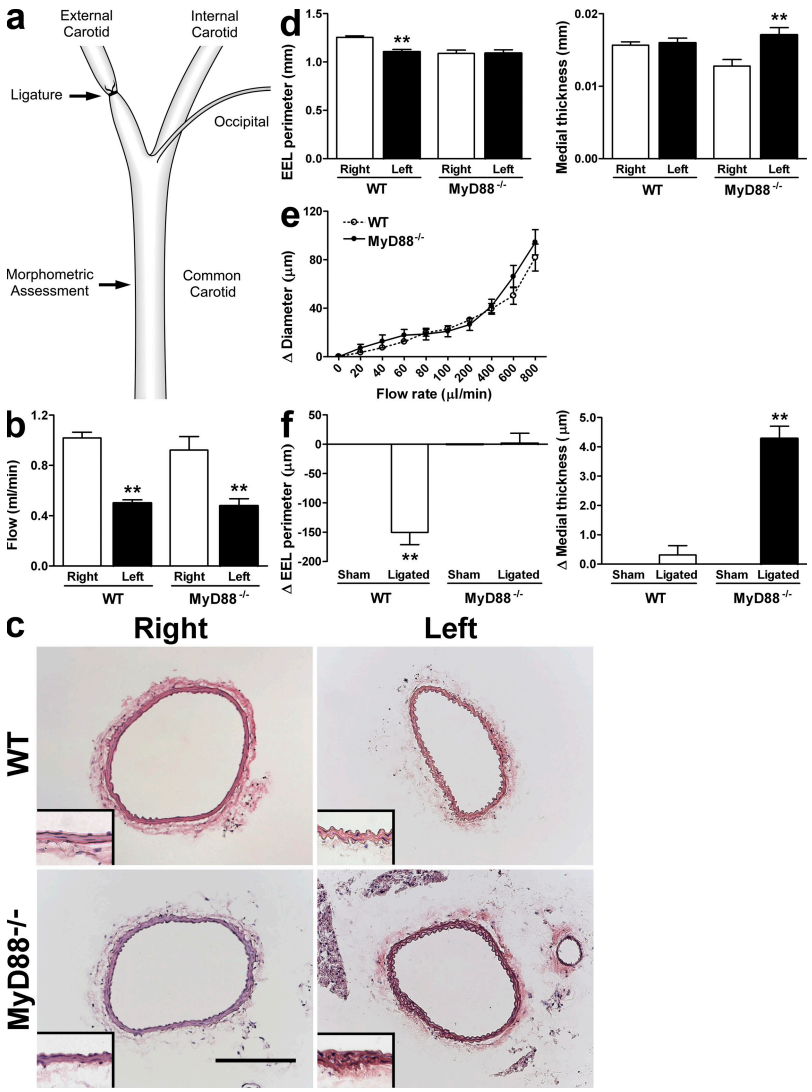

Figure 1. MyD88 is necessary for flow-mediated inward vascular remodeling. (a) The experimental model entailed ligation of the left external carotid artery which limited outflow of blood to the internal carotid and occipital arteries, and morphometric assessment and flow studies at the midpoints of both common carotid arteries was performed after 2 wk. (b) Blood flow within the common carotid arteries was measured by a Doppler probe (n = 8–10). (c) Representative photomicrographs of H&E-stained transverse sections of the right (unligated side) and left (ligated side) common carotid arteries. Bar, 200 μm. Insets depict twofold higher magnification views of the vessel wall. (d) Vessel size (EEL perimeter) and wall (medial) thickness was determined by microscopy and image analysis software (n = 10). (e) Flow-induced changes in vessel size were measured in common carotid arteries ex vivo (n = 3). (f) Changes in EEL perimeter and medial thickness were also determined in left versus right common carotid arteries 2 wk after sham surgery and compared with that of ligation operations (n = 10). Data are means ± SE. *, $P < 0.05$; **, $P < 0.001$, Left versus Right or Sham versus Ligated.

atrophy was characterized by decreased immunoreactivity for α-smooth muscle actin (α-SMA). However, because of the reduction in the size of the medial compartment, the numbers of SMCs per unit volume (i.e., cell density) was basically unchanged. Conversely, there were more medial cells in the inner lamellar units of remodeling vessels in MyD88$^{-/-}$ mice. SMC size was not altered, nor were there significant changes in medial elastin or collagen content in the common carotid arteries of either strain.

We excluded several potential confounding factors for the differences in vessel phenotypes. Mechanosensor function was intact in carotid arteries from MyD88$^{-/-}$ mice as measured by an ex vivo assay of flow-dependent vasomotor responses (Fig. 1 e). The vascular changes were not caused by the surgical procedure, as common carotid artery morphology was unaltered after sham ligation in both WT and MyD88$^{-/-}$ mice (Fig. 1 f). Maladaptive vascular remodeling was not secondary to an immunodeficient state because inward remodeling occurred in recombination-activating gene (RAG)1$^{-/-}$ mice and Trif^{Lps2} mutant mice with defects in adaptive immunity or TLR3 and TLR4 signaling, respectively, albeit with modest medial thickening in the latter

Table I. Medial remodeling of common carotid arteries after outflow reduction

	WT		MyD88$^{-/-}$	
	Right	Left	Right	Left
Medial lamellar units (number)	3.0 ± 0	2.4 ± 0.2[a]	3.0 ± 0	3.0 ± 0
Inner lamella nuclei (per x-sec)	39.2 ± 1.5	38.8 ± 0.6	41.0 ± 1.1	43.2 ± 1.0
Middle lamella nuclei (per x-sec)	36.8 ± 1.6	36.7 ± 1.3	36.2 ± 1.2	39.7 ± 1.4[a]
Outer lamella nuclei (per x-sec)	23.8 ± 2.0	17.8 ± 2.8[a]	27.9 ± 1.1	25.2 ± 2.6
Medial nuclei density (per $\mu m^2 \times 10^3$)	5.0 ± 0.2	4.9 ± 0.2	4.1 ± 0.1	4.7 ± 0.1
Inner lamella SMC size (μm)	6.0 ± 0.1	5.9 ± 0.1	6.5 ± 0.3	6.7 ± 0.2
Middle lamella SMC size (μm)	5.6 ± 0.2	5.7 ± 0.2	6.4 ± 0.2	6.5 ± 0.3
Outer lamella SMC size (μm)	3.7 ± 0.2	3.4 ± 0.3	5.1 ± 0.2	4.7 ± 0.3
Medial α-SMA$^+$ area ($\mu m^2 \times 10^3$)	17.1 ± 0.7	14.7 ± 0.3[a]	17.5 ± 0.9	16.1 ± 0.5
Medial elastin$^+$ area ($\mu m^2 \times 10^3$)	13.1 ± 0.5	12.4 ± 0.5	12.9 ± 0.7	13.0 ± 0.8
Medial sirius red$^+$ area ($\mu m^2 \times 10^3$)	9.6 ± 0.6	9.6 ± 0.7	12.0 ± 1.2	13.0 ± 0.7

Common carotid arteries were formalin fixed and paraffin embedded at 14 d after left external carotid artery ligation in WT and MyD88$^{-/-}$ mice (n = 9). The number of medial lamellar units continuous around >50% of the vessel circumference and the number of nuclei in each lamella were counted from H&E-stained cross sections (x-sec). The transverse diameter of SMCs was measured across the nucleus in sections immunostained for α-SMA. The medial area staining positive for α-SMA, elastin, or Sirius red was calculated using image analysis software. Data are means ± SE.
[a]$P < 0.05$, Left versus Right.

strain (Fig. S3 a, available at http://www.jem.org/cgi/content/full/jem.20081298/DC1). Although the common carotid arteries were smaller in MyD88$^{-/-}$ compared with WT mice, there was a comparable difference in body size (Fig. S3 b). Furthermore, vessels from older and larger MyD88$^{-/-}$ mice also failed to inwardly remodel, but displayed medial thickening in response to flow reduction (Fig. S3 c). Finally, thrombus, which may modulate vascular remodeling responses, was not noted in any artery specimen on macroscopic examination or in the ligated left external carotid artery on microscopic examination (Fig. S3 d).

Flow reduction is associated with cytokine production within the vessel wall

Having established that flow-mediated vascular remodeling is dependent on MyD88, a well-characterized signal transducer for innate immune responses, we next investigated whether vascular inflammatory responses were induced by decreased blood flow. Quantification of transcript expression within common carotid arteries revealed that several cytokines and chemokines, such as IL-1β, IL-6, IFN-γ–induced protein of 10 kD (IP-10, also known as CXCL10), and monokine induced by γ-IFN (Mig, also known as CXCL9), were rapidly induced by 6 h after outflow reduction, whereas other inflammatory mediators, such as TNF-α and inducible (i)NOS, peaked later at 3 d after external carotid artery ligation (Fig. 2 a). Increases in cytokine transcripts were not observed after sham operations (unpublished data). We confirmed an increase in IL-1β protein expression at 24 h by ELISA, and immunohistochemical analysis also demonstrated expression of IL-1β in the endothelium and media of arteries with reduced outflow (Fig. 2, b and c). Additionally, plasma levels of IL-1β were higher in mice 24 h after external carotid artery ligation versus sham operations. The detection of phospho-p65 immunoreactivity at an earlier time point of 3 h was consistent with NF-κB activation as a link between MyD88 signaling and cytokine synthesis.

Flow-induced superoxide generation is dependent on MyD88

To gain insight into flow-initiated vascular inflammation, we investigated the role of factors that may lead to or respond to MyD88-dependent signaling. The expression of several TLRs that signal via MyD88 and/or TRIF, including TLR4, were not essential for flow-mediated inward vascular remodeling (Fig. S4 a, available at http://www.jem.org/cgi/content/full/jem.20081298/DC1). Furthermore, MyD88-dependent signaling by IL-1 and -18 was not required, as inward remodeling occurred after external carotid artery ligation in IL-1β converting enzyme (ICE)$^{-/-}$ and IL-1R$^{-/-}$ mice.

We next examined the role of superoxide because it is induced in vascular cells after flow disturbances and is also required for certain innate immune responses (18, 36). We established a method to measure superoxide activity in vivo using HPLC to detect oxidant-dependent products of the fluorogenic probe, dihydroethidium (DHE), which is described as the gold standard for ROS detection in cardiovascular studies (37). DHE was applied to the adventitia of common carotid arteries together with the superoxide generator menadione. The superoxide-dependent product 2-hydroxyethidium and the superoxide-independent product ethidium were detected in artery extracts after 6 h (Fig. 3 a). The presence of these oxidative products was dampened by tempol, which is an SOD mimetic agent. We then extended this method to our flow-mediated vascular remodeling studies. After topical application of DHE to both common carotid arteries and ligation of the left external carotid artery, 2-hydroxyethidium was only detected in vessel extracts from

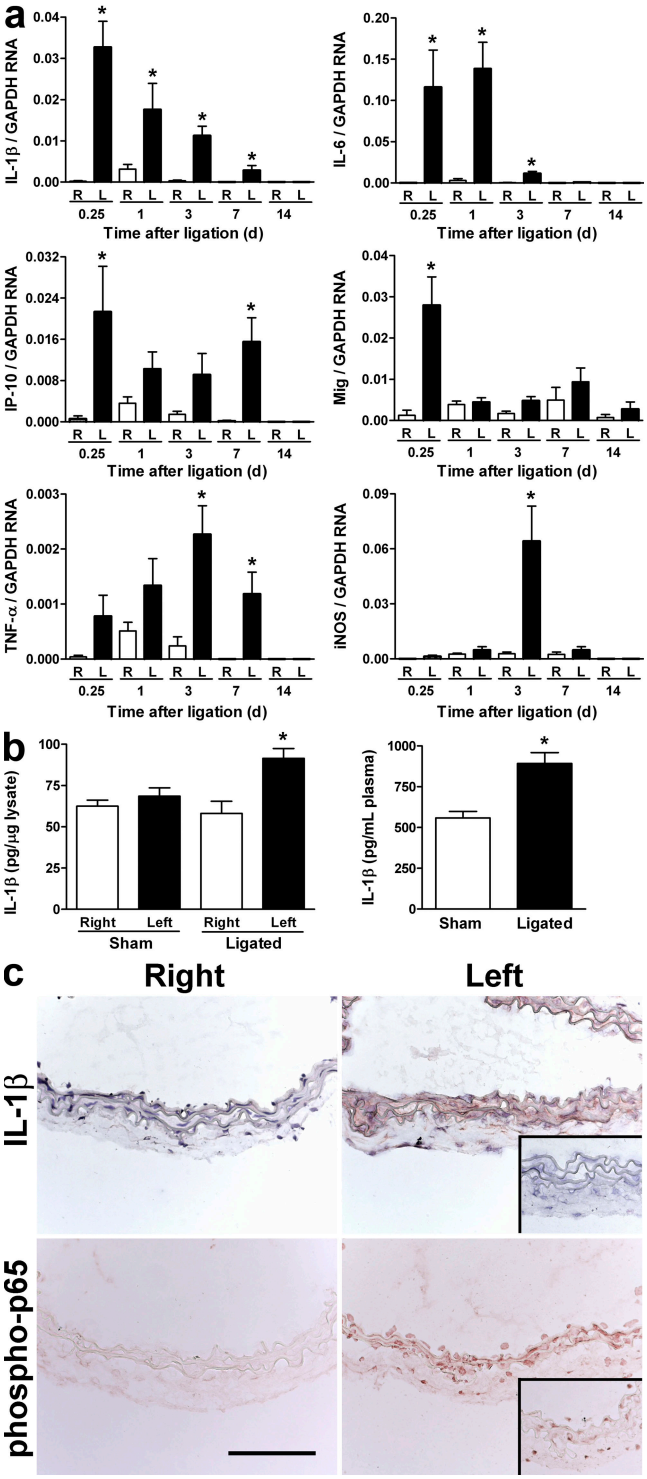

Figure 2. Flow reduction is associated with cytokine production within the vessel wall. (a) Transcripts for IL-1β, IL-6, IP-10, Mig, TNF-α, and iNOS were quantified by qRT-PCR and normalized to GAPDH from right (R) and left (L) common carotid artery lysates of WT versus MyD88$^{-/-}$ mice at 6 h (n = 10), 1 d (n = 8), 3 d (n = 9), 7 d (n = 11), and 14 d (n = 6) after left external carotid artery ligation. (b) IL-1β protein was measured by ELISA in common carotid artery lysates and plasma at 24 h after sham operations or left external carotid artery ligation (n = 6). Data are means ± SE, *P < 0.05 and **P < 0.001, Left versus Right or Sham versus Ligated. (c) Representative photomicrographs of IL-1β and phospho-p65 immunoreactivity (colored brown) in right (unligated side) and left (ligated side) common carotid artery sections at 24 and 3 h after outflow reduction, respectively. Bar, 100 μm. Control immunostaining with isotype-matched, irrelevant antibody is shown in inset (top), and NF-κB activation after topical application of lipopolysaccharide at 0.5 mg/ml for 3 h is demonstrated in inset (bottom).

the ligated side and threefold more ethidium was detected from the ligated versus unligated sides at 6 h (Fig. 3 b). There was an associated increase of DHE in ligated (and menadione-treated) arteries of WT mice compared with control vessels (Fig. S4 b). The detection of 2-hydroxyethidium was specifically inhibited by tempol. In contrast, no 2-hydroxyethidium and only low levels of ethidium were detected in common carotid artery extracts of MyD88$^{-/-}$ mice after outflow ligation (Fig. 3 b). The lack of superoxide detection in both tempol-treated WT mice and in MyD88$^{-/-}$ mice was not caused by decreased vessel concentrations of DHE (Fig. S4 b). These results suggest that flow-induced ROS production was dampened or prevented in the absence of MyD88.

Inhibition of superoxide prevents flow-mediated vascular inflammatory responses and remodeling

In turn, we investigated if ROS were necessary for MyD88-dependent vascular changes after outflow ligation. Tempol inhibition of superoxide activity prevented the induction of IL-1β transcripts in common carotid arteries from the ligated side at 6 h (Fig. 3 c). Similar results were achieved with a mitochondria-targeted form of the drug, mito-tempol as well as with rotenone, an inhibitor of superoxide generation from the respiratory chain. We also tested other potential sources of ROS. Administration of apocynin, widely used as a NADPH oxidase inhibitor, partially reduced the accumulation of IL-1β transcripts at 6 h. However, inhibition of xanthine oxidase with allopurinol or endothelial (e)NOS with L-NAME did not influence IL-1β production. As pharmacological approaches may have off-target effects, we also used genetic strategies to investigate the effects of superoxide. The expression of IL-1β was partially decreased after external carotid artery ligation in transgenic mice overexpressing SOD2, the mitochondrial isoform of SOD (Fig. 3 c). There was a similar partial reduction of inflammatory responses in mice with EC-specific overexpression of the mitochondrial antioxidant, thioredoxin (TXN)2 and in p47$^{phox-/-}$ mice with defective NADPH oxidase activity. Superoxide inhibition also resulted in variable and incomplete suppression of other proinflammatory factors induced at 6 h (Fig. 3 d). Cumulatively, these data point to a key role of ROS in general, and superoxide in particular, in mediating the generation of proinflammatory cytokines and chemokines by vessel wall cells in response to decreased flow in WT mice. Moreover, the inhibition of vascular inflammatory responses

using rotenone in WT mice, SOD2 transgenic mice, and p47$^{phox-/-}$ mice prevented inward vascular remodeling and allowed for increased medial thickening after outflow reduction (Fig. 3 e).

Flow reduction is associated with transient perivascular leukocytic infiltrates

We then investigated if vascular production of cytokines and chemokines resulted in leukocyte recruitment. The temporal expression of transcripts for the pan-leukocyte marker CD45 and the macrophage marker F4/80 trailed those of IL-1β, IL-6, IP-10, and Mig, and coincided with those of TNF-α and iNOS (Fig. 4 a). Immunohistochemical analysis verified adventitial infiltration by CD45$^+$ and F4/80$^+$ cells and established that macrophages accounted for 80–90% of infiltrating leukocytes with maximal accumulation at 3–7 d and resolution by 14 d after external carotid artery ligation (Fig. 4, b and c). The expression of transcripts for the T cell marker CD3ε and the dendritic cell marker CD11c, but not that of the neutrophil markers, myeloperoxidase and Gr-1, were also detected in ligated vessel lysates (Fig. S5 a, available at http://www.jem.org/cgi/content/full/jem.20081298/DC1). Immunostaining demonstrated that CD3$^+$ T cells and CD11c$^+$ dendritic cells constituted a minor population of infiltrating CD45$^+$ cells (Fig. S5, b–d). To further investigate the mechanisms for adventitial accumulation of leukocytes, we assessed

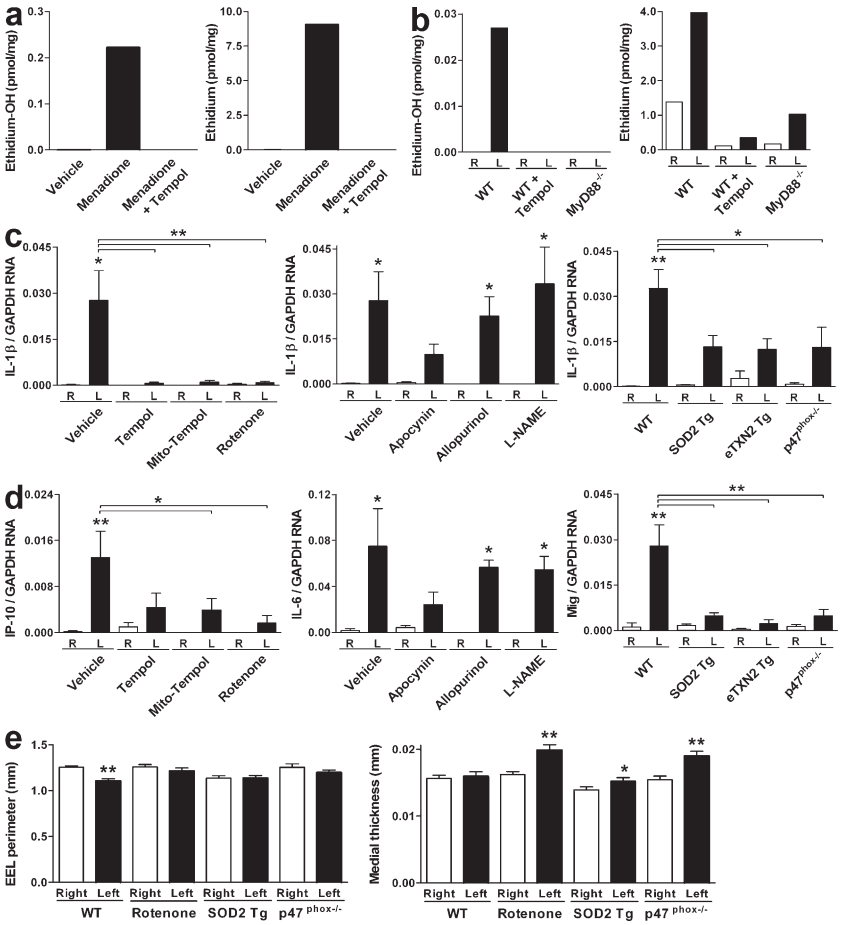

Figure 3. Flow-induced generation of superoxide is MyD88-dependent and is necessary for vascular inflammatory responses and inward remodeling. (a) 2-Hydroxyethidium (ethidium-OH) and ethidium were detected by HPLC at 6 h after topical application of menadione versus vehicle together with DHE to common carotid arteries. Each group represents six pooled vessel extracts. The determinations were also performed after i.p. administration of tempol. (b) 2-Hydroxyethidium and ethidium were detected in left, but not right, common carotid arteries at 6 h after left external carotid artery ligation in WT mice. Each group represents six pooled vessel extracts. Both oxidant products were suppressed by tempol treatment. No 2-hydroxyethidium and minimal ethidium were detected in pooled vessel extracts from MyD88$^{-/-}$ mice. The data are representative of two independent experiments. (c) IL-1β transcripts were measured by qRT-PCR and normalized to GAPDH in right (R) and left (L) common carotid arteries at 6 h after left external carotid artery ligation and systemic administration of vehicle, tempol, mito-tempol, rotenone, apocynin, allopurinol, and L-NAME to WT mice or no treatment in WT, SOD2 transgenic (Tg), EC-specific (e)TXN2 transgenic, and p47$^{phox-/-}$ mice. (d) Similarly, IL-6, IP-10, and Mig transcripts were analyzed after pharmacologic and genetic inhibition of superoxide. (e) Vessel size (EEL perimeter) and wall (medial) thickness were determined at 2 wk after outflow reduction in untreated WT, rotenone-treated WT, SOD2 transgenic, and p47$^{phox-/-}$ mice. Data are means ± SE (n = 8–10). *, P < 0.05; **, P < 0.001, Left versus Right or Superoxide Inhibition versus Vehicle/WT.

the expression of adhesion molecules in the vessel wall. At 1 d after left external carotid artery ligation, before maximal leukocytic infiltration, vascular cell adhesion molecule (VCAM)-1 expression was induced both on carotid intimal ECs and on adventitial microvascular ECs (Fig. S5 e). This expression pattern paralled that of IL-1β at the same time point and confirmed a transmural inflammation of the vessel wall in response to reduced blood flow.

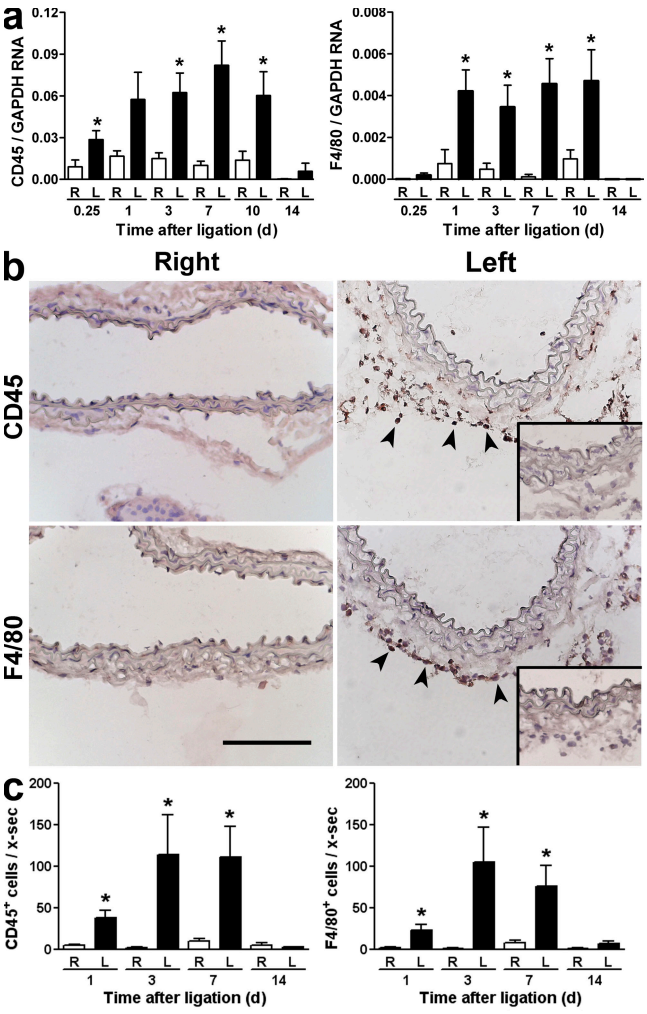

Figure 4. Flow reduction is associated with transient perivascular leukocytic infiltrates. (a) CD45 (pan-leukocyte marker) and F4/80 (macrophage marker) transcripts from right (R) and left (L) common carotid artery lysates were quantified by qRT-PCR and normalized to GAPDH at 6 h (n = 10), 1 d (n = 8), 3 d (n = 9), 7 d (n = 11), 10 d (n = 7), and 14 d (n = 6) after left external carotid artery ligation. (b) Representative photomicrographs of CD45 and F4/80 immunostaining (brown, arrowheads) in right (unligated side) and left (ligated side) common carotid artery sections at 3 d after outflow reduction. Bar, 100 µm. Immunoreactivity of isotype-matched, irrelevant antibodies is shown in the insets. (c) $CD45^+$ and $F4/80^+$ cells infiltrating the adventitia of common carotid artery cross sections (x-sec) were counted at 1 d (n = 5), 3 d (n = 8), 7 d (n = 8), and 14 d (n = 7) postoperatively. Data are means ± SE. *, $P < 0.05$; **, $P < 0.001$, Left versus Right.

Macrophage depletion prevents flow-mediated inward vascular remodeling

To directly test if macrophages played a causal role in the remodeling process, we selectively depleted phagocytes by systemic administration of clodronate liposomes. This strategy depleted 80% of circulating monocytes (Fig. 5 a) and markedly diminished common carotid artery–infiltrating $F4/80^+$ cells and iNOS production after outflow reduction (Fig. 5, b and c). The recruitment of $CD45^+$ leukocytes and the induction of TNF-α was minimally affected, suggesting that this cytokine was produced by cells other than macrophages, e.g., T cells. Successful macrophage depletion prevented inward vascular remodeling and resulted in medial thickening after external carotid artery ligation compared with administration of vehicle-containing liposomes (Fig. 5 d). These findings

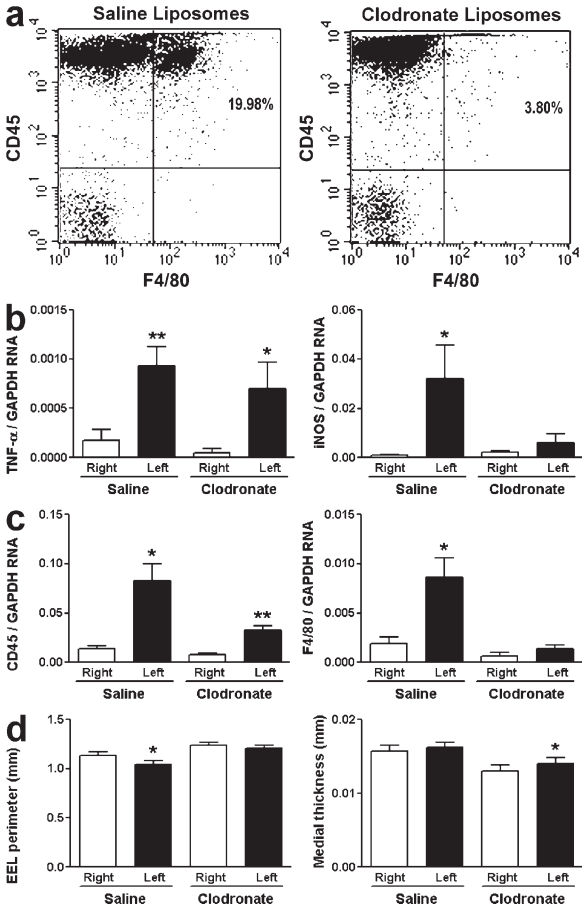

Figure 5. Macrophage depletion prevented inward vascular remodeling. (a) The frequency of circulating leukocytes expressing CD45 and F4/80 was analyzed by flow cytometry after administration of clodronate- versus vehicle-containing liposomes for 3 wk, starting 1 wk before external carotid artery ligation. TNF-α (b), iNOS, CD45 (c), and F4/80 transcript expression and vessel size (d; EEL perimeter) and wall (medial) thickness were determined after liposome treatment at 3 and 14 d postoperatively, respectively. Data are means ± SE (n = 9–10). *, $P < 0.05$; **, $P < 0.001$, Left versus Right.

indicate an essential role for recruited macrophages in flow-mediated inward vascular remodeling.

Flow-initiated vascular inflammation is dependent on MyD88

Having established that there are transient inflammatory responses in arteries of WT mice subjected to flow reduction, we evaluated these events in common carotid arteries of MyD88$^{-/-}$ animals. The expression of IL-1β, IL-6, IP-10, and Mig transcripts was either not detected or not up-regulated between vessels from ligated versus unligated sides at 6 h in MyD88$^{-/-}$ mice (Fig. 6 a). Similarly, the production of TNF-α and iNOS was also inhibited at 3 d (Fig. 6 b). Myd88 deficiency did not prevent recruitment of CD45^{+} and F4/80^{+} cells at 3 d (Fig. 6 c), but attenuated inflammation within the vessel wall at 7 d (Fig. 6 d). These results imply that MyD88 is required for vascular inflammatory responses, as well as for macrophage activation and later accumulation, but is not essential for the initial recruitment of leukocytes after outflow reduction.

Vascular cell and leukocyte expression of MyD88 are required for flow-mediated inward vascular remodeling

Our data suggest distinct effects of MyD88 on early events (vascular ROS and cytokine/chemokine generation) and on

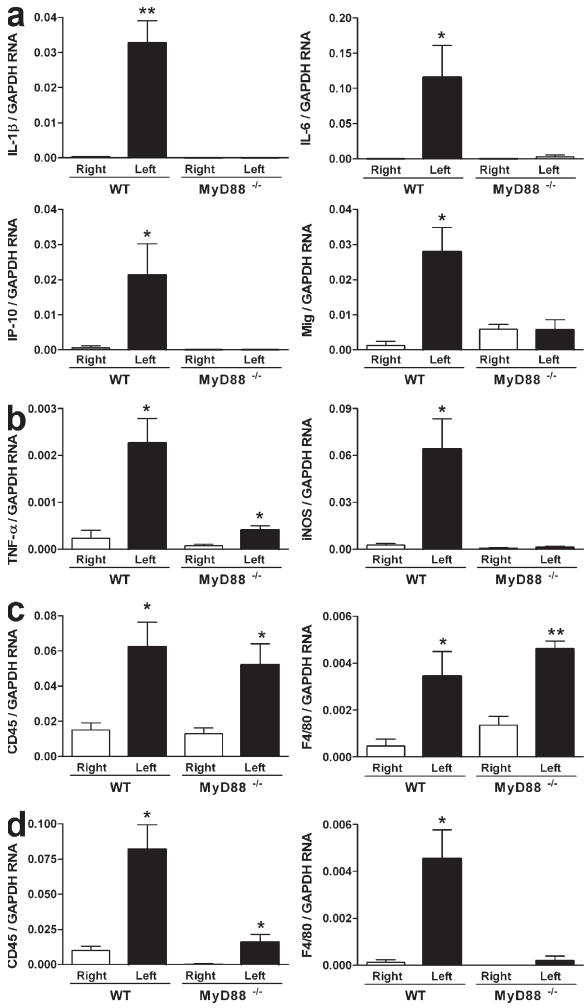

Figure 6. MyD88 is necessary for flow-mediated vascular inflammation and macrophages are essential for flow-mediated vascular remodeling. (a) Transcripts for IL-1β, IL-6, IP-10, and Mig from right and left common carotid artery lysates of WT versus MyD88$^{-/-}$ mice were quantified by qRT-PCR and normalized to GAPDH at 6 h after left external carotid artery ligation. Similarly, transcripts were measured for TNF-α and iNOS at 3 d (b), as well as for CD45 and F4/80 at 3 (c) and 7 (d) days post-operatively. Data are means ± SE (n = 8–10). *, P < 0.05; **, P < 0.001, Left versus Right.

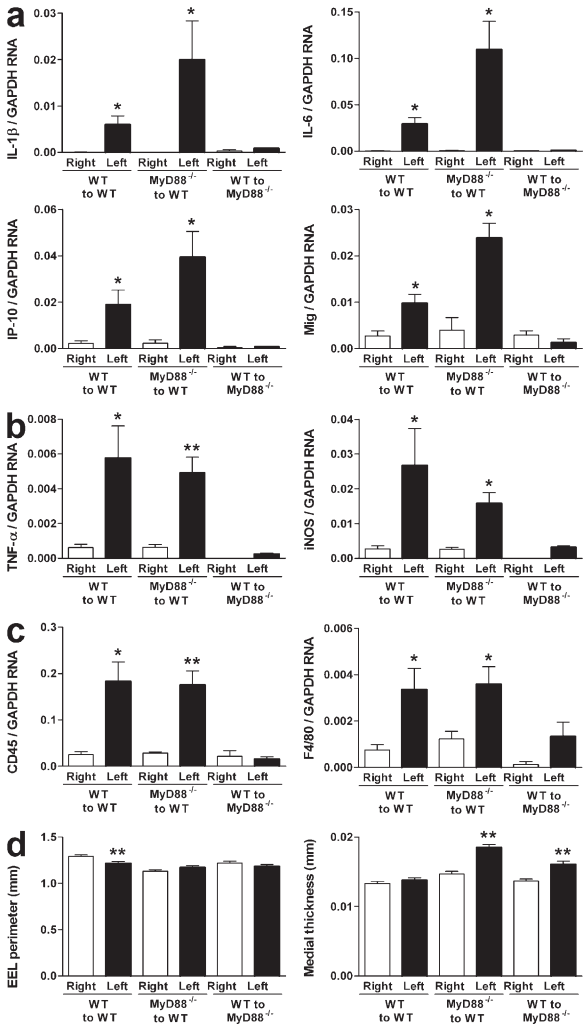

Figure 7. Vascular cell and leukocyte expression of MyD88 are required for flow-mediated vascular inflammation and vascular remodeling, respectively. (a) Transcripts for IL-1β, IL-6, IP-10, and Mig from right and left common carotid artery lysates of WT to WT, MyD88$^{-/-}$ to WT, and WT to MyD88$^{-/-}$ BM chimeras were quantified by qRT-PCR and normalized to GAPDH at 6 h after left external carotid artery ligation. Similarly, TNF-α (b), iNOS, CD45 (c), and F4/80 transcripts were measured at 3 d post-operatively. (d) Vessel size (EEL perimeter) and wall (medial) thickness at 2 wk after outflow reduction. Data are means ± SE (n = 9–12). *, P < 0.05; **, P < 0.001, Left versus Right.

later events (macrophage persistence, iNOS production, and vascular remodeling) in our model. We used BM reconstitution experiments to characterize which cell types required MyD88 expression for flow-mediated vascular inflammation and inward remodeling. The detection of IL-1β, IL-6, IP-10, and Mig transcripts at 6 h in MyD88$^{-/-}$ BM to WT chimeras, but not in WT BM to MyD88$^{-/-}$ chimeras, established that vascular cell expression of MyD88 was necessary for these early inflammatory responses (Fig. 7 a). The subsequent expression of TNF-α and iNOS transcripts at 3 d was preserved in MyD88$^{-/-}$ BM to WT chimeras, but was markedly reduced in WT to MyD88$^{-/-}$ mice (Fig. 7 b). Cytokine production within the vessel wall was associated with macrophage recruitment at 3 d in MyD88$^{-/-}$ BM to WT chimeras and conversely decreased cytokine synthesis correlated with significantly fewer infiltrating leukocytes in WT BM to MyD88$^{-/-}$ chimeras (Fig. 7 c). These results indicated that flow-induced vascular cytokine/chemokine production and leukocyte recruitment were independent of MyD88 expression in BM-derived cells. However, MyD88 expression by both intrinsic vascular cells and infiltrating leukocytes was required for flow-dependent inward vascular remodeling because this did not occur in either MyD88$^{-/-}$ BM to WT or WT BM to MyD88$^{-/-}$ chimeras (Fig. 7 d). A maladaptive vascular phenotype was supported by evidence of abnormal medial thickening in both of these groups.

DISCUSSION

Our findings define an essential role for inflammation in flow-mediated inward vascular remodeling of conduit arteries. Decreased arterial blood flow after partial outflow ligation leads to vessel shrinkage through nonredundant MyD88-dependent effects, viz. superoxide generation, vascular cytokine and chemokine production, and transient macrophage accumulation and activation. It is generally accepted that physiological flow-mediated vascular remodeling and pathological immune-mediated vascular remodeling are distinct processes. Instead, our work supports the concept that inflammation is necessary for adaptive vascular remodeling in response to hemodynamic forces.

The degree and kinetics of inward vascular remodeling, as well as the unchanged medial thickness with medial atrophy that we observe in WT mice, is similar to that of previous studies using the external carotid artery ligation technique (4, 35, 38). In this model, reversible vasoconstriction accounted for early arterial diameter changes up to 3 d after outflow reduction, whereas vasodilator-resistant structural changes were noted by day 7 (38). Coincident with the permanent medial remodeling, a loss of SMCs was documented together with an increased rate of cell death as measured by propidium iodide uptake (38). Our observation of cell loss primarily in the outermost medial lamellar unit of the ligated vessel is consistent with our hypothesis of vascular remodeling in response to adventitial inflammation. The contrasting phenotype of increased medial thickness and medial expansion after decreased blood flow in MyD88$^{-/-}$ mice is surprising. Outflow ligation should not increase blood pressure locally to account for unilateral medial expansion. Unchanged vessel size with medial thickening are also found after inhibition of superoxide or depletion of macrophages in our study, and similar findings have been reported in ligated arteries of eNOS$^{-/-}$, caveolin-1 (Cav1)$^{-/-}$, and β1 integrin$^{-/-}$ mice with defective mechanotransduction function (35, 39, 40). Characterization of the medial hyperplasia in these latter strains demonstrated an increased rate of cellular proliferation as measured by 5-bromo-2'deoxyuridine incorporation (35, 39). Medial expansion may represent a form of dysregulated vascular remodeling to decreased shear stress when normal adaptation in vessel size is prevented. In contrast to adaptive remodeling, this maladaptive change occurs in the absence of MyD88 and involves the inner rather than the outer medial lamellar units. If it, too, is dependent on inflammation, a subject of future studies, this finding implies that the mechanisms underlying these processes are distinct as shown by the differential role of MyD88.

The time period during which active shrinkage of vessel size occurs from postoperative days 3–7 coincides temporally with peak macrophage accumulation and monokine production. Furthermore, the inflammation resolves within a few days of permanent adaptations for abnormal shear stresses, i.e., by 14 d after external carotid artery ligation. The transient nature of the inflammatory responses may explain why they have been overlooked in previous studies of external carotid artery ligation. In models of more severe outflow obstruction caused by combined internal and external carotid artery ligation, persistent vascular inflammation is detected at 2 wk and is associated with neointima formation (30, 31). The inflammatory changes and intimal expansion are even more pronounced in models of complete outflow obstruction after ligation of the common carotid artery that are associated with thrombosis (32, 33). These experimental models with very low flow or no flow are useful in reproducing conditions of diseased vessels, but provide limited insight into mechanisms of physiological vascular remodeling. We are uncertain whether our findings will apply to models of outward vascular remodeling of conduit arteries, as it has been previously documented that monocyte adhesion to the endothelium of common carotid arteries is induced by low, but not high, shear stresses (28). In contrast, adventitial infiltration by macrophages has recently been noted after both increased and absent flow in smaller mouse mesenteric resistance arteries (34).

We detect SOD-inhibitable, superoxide-specific, and other oxidant-dependent products in common carotid arteries after ipsilateral external carotid artery ligation in WT, but not in MyD88$^{-/-}$ mice. A confounding variable in the interpretation of our HPLC results is that menadione treatment or outflow ligation is associated with an increased intracellular level of DHE probe in vascular cells after 6 h compared with untreated or unligated vessels. This may reflect the superoxide-dependent, NF-κB–mediated inflammatory responses of ECs spreading to underlying SMCs and manifesting as increased uptake or altered consumption of DHE. The mechanisms responsible

for changes in intracellular DHE levels are currently under investigation. Similar caveats to the interpretation of this method of superoxide detection also apply to in vitro systems (41). Despite these methodologic limitations, the absence of superoxide detection in the face of detectable DHE after systemic tempol treatment in WT mice or after outflow reduction in MyD88$^{-/-}$ mice is compelling. Our pharmacological and genetic studies suggest that both mitochondrial respiratory chain and NADPH oxidase sources of superoxide play at least partial roles in flow-induced vascular inflammation and remodeling. This is consistent with the view of mitochondria as signaling organelles in ECs (12) and previous observations of interactions between mitochondrial ROS and NADPH oxidases (13). An alternative interpretation of the results is that antioxidant strategies in mitochondrial versus cytosolic and membrane locations act as superoxide sinks and may inhibit ROS required for physiological signaling in remote cellular compartments. Prior studies have shown that shear stress increases NADPH oxidase activity in ECs (18, 42) and that superoxide activates endothelial NF-κB and induces monocyte adhesion (43, 44). We extend these findings by demonstrating that superoxide generation in response to low shear stress is attenuated in the absence of MyD88, and that superoxide activity contributes to MyD88-dependent vascular inflammatory responses induced by reduced flow. Additionally, the observation of diminished cytokine production after external carotid artery ligation in mice with EC-specific overexpression of TXN2 suggests a primary role for the endothelium in flow-mediated, superoxide-dependent inflammatory responses.

The mechanisms linking endothelial mechanosensors to MyD88-dependent vascular inflammatory responses, as well as MyD88-dependent macrophage functions to structural vascular remodeling also remain unclear. MyD88-dependent signaling by TLRs, IL-1β, and IL-18 does not appear to be essential, although individual TLRs may have redundant roles or other TLRs than those we investigated may provide a mechanistic link. Caveolae and eNOS mechanotransduction may be of importance in this context, as our preliminary investigations demonstrate blunted cytokine production in Cav1$^{-/-}$ and eNOS$^{-/-}$ mice after external carotid artery ligation (unpublished data). Interestingly, MyD88 is known to be enriched in Cav1-associated lipid raft microdomains (45), and MyD88 activity is modulated by eNOS-dependent nitrosylation (46). However, direct activation of MyD88 by endothelial mechanosensors, such as P2X4 ion channels (47) and platelet-EC adhesion molecule-1 (48) cannot be excluded. It is also possible that the MyD88-dependent effects we observe are not directly related to mechanotransduction signaling pathways, but rather to transcript instability in the absence of MyD88 expression, as described for IFN-γ–inducible molecules (24), which could lead to an altered setpoint for vascular cells to shear stress–initiated inflammatory responses.

Our observations regarding macrophage recruitment versus activation and accumulation are consistent with previous reports that MyD88 deficiency impairs monocyte activation and pathogen clearance, but not mononuclear cell trafficking, to sites of certain bacterial and spirochetal infections (49–51). Specifically, in a murine model of *Listeria monocytogenes* infection, the initial recruitment of macrophages was caused by MyD88-independent production of MCP-1. Similarly, MyD88-independent generation of chemokines, other than those we studied, or other chemotactic agonists, such as lipid chemoattractants, may have contributed to early monocyte recruitment in our model. Our results indicate that MyD88-dependent vascular inflammatory responses are necessary for macrophage activation, as indicated by iNOS synthesis, but not for initial leukocyte recruitment after outflow ligation. We cannot tell from the current experiments whether macrophage persistence depends on MyD88-dependent vascular inflammation or on MyD88-dependent macrophage activation. Macrophages are known to facilitate the remodeling of murine resistance arteries after deoxycorticosterone- or angiotensin-induced hypertension and vascular injury and after flow cessation in ligated mesenteric vessels through undefined mechanisms (34, 52, 53). Our ongoing investigations indicate that iNOS production by macrophages is not required for flow-mediated inward vascular remodeling (unpublished data). Other candidate macrophage-derived molecules that may be responsible for structural vascular reorganization include matrix metalloproteinase-9, which is required for extracellular matrix degradation in outward remodeling of mouse carotid arteries (33), and coagulation factor XIII, which is a transglutaminase associated with extracellular matrix cross-linking during inward remodeling of mouse mesenteric arteries (54).

We conclude that decreases in endothelial shear stress activate vascular stress responses that signal via cytokines and chemokines to elicit transient inflammation that is essential for inward vascular remodeling and the restoration of normal hemodynamic forces. MyD88 is a central mediator of this process with superoxide a key intermediary. Adventitial, unlike intimal, accumulation of macrophages may result in adaptive vascular responses without necessarily causing vascular disease. These physiological events may contribute to lumen loss and ischemia in obstructive arterial disease, which is the leading cause of death and disability. A homeostatic role for inflammation may also apply to the responses of other tissues to physical forces.

MATERIALS AND METHODS

Mice. We purchased C57BL/6, RAG1$^{-/-}$, TLR2$^{-/-}$, IL-1R$^{-/-}$, and p47$^{phox-/-}$ mice from The Jackson Laboratory. We obtained MyD88$^{-/-}$ mice from S. Akira (Osaka University, Osaka, Japan); ICE$^{-/-}$, TLR3$^{-/-}$, and TLR7$^{-/-}$ mice from R.A. Flavell (Yale University, New Haven, CT); TLR4$^{-/-}$ mice from P.J. Lee (Yale University, New Haven, CT); Trif^{Lps2} mutant mice from B. Beutler (The Scripps Research Institute, La Jolla, CA); SOD2 transgenic mice from A.G. Richardson (University of Texas, San Antonio, Texas); and CD45.1 C57BL/6 mice from the National Cancer Institute. The generation of EC-specific TXN2 transgenic mice has been previously described (55). All strains had been backbred to a C57BL/6 background for >10 generations. Vessel procedures were performed in 8–12-wk-old male mice, except for the experiments in older recipients and in BM chimeras, which were performed in 18–22-wk-old male mice.

External carotid artery ligation. All animal studies were approved by the Yale University Animal Care and Use Committee. After anesthesia, the left external carotid artery was isolated and ligated with a 6–0 silk suture (United States Surgical) through a midline cervical incision (35, 38). For sham operations, a suture was tied around the artery in a nonconstricting fashion. The wound was closed with a 5–0 prolene suture. For morphometry and immunohistochemistry studies, the left and right common carotid arteries were harvested after perfusion fixation with 4% paraformaldehyde in phosphate-buffered saline at a mean pressure of 100 mmHg through the left ventricle and immediately embedded in Optimal Cutting Temperature medium (Tissue-Tek). For medial remodeling studies, the perfusion-fixed vessels were post-fixed overnight in 10% formalin and embedded in paraffin for optimal histological details of SMCs and extracellular matrix. For ELISA, RT-PCR, and HPLC studies, the right and left common carotid arteries were isolated after saline perfusion and snap frozen.

Morphometric analysis. Morphometric analysis was performed from hematoxylin and eosin (H&E)–stained sections of Optimal Cutting Temperature medium–embedded specimens using computer-assisted microscopy. Internal elastic lamina perimeter, external elastic lamina (EEL) perimeter, and medial thickness at four quadrants were measured and averaged over 10 separate sections using an image software program (ImageJ; National Institutes of Health). The number of nuclei in each medial lamellar unit and the number of medial lamellar units continuous around the majority (>50%) of the circumference were counted in H&E-stained sections of paraffin-embedded specimens. The transverse diameter of SMCs was measured across the nucleus using image analysis software and averaged from 20 cells in sections immunostained for α-SMA (56). The medial area staining positive for α-SMA, elastin Van Gieson, and Sirius red (as a measure of SMC contractile protein, extracellular elastin, or extracellular collagen, respectively) was calculated using image analysis software (57).

Flow measurement. After anesthesia, a midline cervical incision was made and the right and left common carotid arteries were exposed. Blood flow was measured at the vessel midpoints using a Doppler flow probe (0.5 mm V-series probe; Transonic Systems Inc.).

Flow-induced vasodilatation. The in vitro assessment of mechanosensor function was as previously described (39). In brief, common carotid artery segments were cannulated at both ends and immersed in Krebs-Ringer solution at 37°C. Intraluminal and extraluminal perfusion with a transmural pressure of 70 mmHg was provided by two separate perfusion pumps. Internal diameters were measured using a binocular loop (Model XC-73; Sony) coupled to a video camera (Living System Instrumentation, Inc.) while pressures were maintained at a constant level using a servo-control during graded increases in flow from 0 to 800 μl/min.

ELISA. Plasma and carotid lysate levels of murine IL-1β were determined using a sandwich ELISA kit (R&D Systems). The lower limit of detection for IL-1β was 15.6 pg/ml.

Immunohistochemistry. Primary antibodies included rat anti–mouse IL-1β (MBL International), F4/80 (Abcam), and CD45 (eBioscience), hamster anti–mouse CD3ε and CD11c (eBioscience), rabbit anti–phospho-Ser276 NF-κB p65 (Cell Signaling Technology), goat anti–mouse VCAM-1 (R&D Systems), mouse anti–α-SMA peptide (Thermo Fisher Scientific), and isotype-matched, nonbinding immunoglobulin. Binding of secondary antibodies (Jackson ImmunoResearch Laboratories) was detected with peroxidase/3-amino ethyl carbazole kits (Vector Laboratories). Cell counting of nuclei surrounded by positive immunostaining was performed under high magnification.

Quantitative (q)RT-PCR. Isolation and DNase-treatment of total RNA was performed using the Nanoprep system (Stratagene), and bulk reverse transcription using random hexamer primers was done using the Multiscribe RT system protocol (Applied Biosystems). Real-time RT-PCR reactions were performed in duplicate using Applied Biosystem Taqman PCR reagents and Taqman gene expression probes for GAPDH, IL-1β, IL-6, IP-10, Mig, TNF-α, iNOS, CD45, F4/80, CD3e, and CD11c. DNase-treated RNA samples produced without RT enzyme were used as negative controls. An iCycler and its system interface software (Bio-Rad Laboratories) were used to analyze the samples and data. Transcript expression levels were normalized to GAPDH.

Macrophage depletion. Mononuclear phagocytes were eliminated by i.v. injection of 200 μl clodronate (also known as dichloromethylene-bisphosphonate) containing liposomes every 3 d, starting 1 wk preoperatively. Clodronate was a gift from Roche. Phosphate-buffered saline–containing liposomes were administered to control animals. Clodronate and saline liposomes were prepared as previously described (58).

BM transplantation. We created WT to WT, MyD88$^{-/-}$ to WT, and WT to MyD88$^{-/-}$ chimeras by irradiating 8–10-wk-old CD45.1 C57BL/6 mice or CD45.2 MyD88$^{-/-}$ mice with 1,000 cGy in two split doses over 4 h from a cesium irradiator. The recipients received 10^7 BM cells isolated from CD45.1 C57BL/6 mice or CD45.2 MyD88$^{-/-}$ mice via tail vein injections. Chimerism was confirmed 12 wk later (at the time of vessel procurement for transcript expression and morphometry studies) by flow cytometric analysis of spleen and lymph nodes cells for reconstitution with donor CD45.1$^+$ or CD45.2$^+$ macrophages.

Pharmacological agents. ROS generation or activity were suppressed in vivo using tempol at 275 mg/kg i.p. (EMD Chemicals, Inc.), mito-tempol at 10 mg/kg i.p. (provided by J. Joseph, Medical College of Wisconsin, Milwaukee, WI), rotenone at 2.5 mg/kg i.p. (VWR International, Inc.), apocynin at 100 mg/kg i.p. (EMD Chemicals, Inc.), allopurinol at 100 mg/kg i.p. (VWR International, Inc.), and L-NAME at 100 mg/kg i.p. (Cayman Chemical Company).

HPLC analysis. DHE (EMD Chemicals) was applied to the adventitial surface of both common carotid arteries at 50 μM in 100 μl saline/1% DMSO after either topical menadione application at 25 mM in 100 μl saline/1% DMSO or immediately after ligation of the left common carotid artery. In certain experiments, tempol was also administered at 275 mg/kg i.p. The wounds were closed and the mice were allowed to recover from anesthesia. After 6 h, the common carotid arteries were procured and snap frozen. Before analysis, the frozen artery sample was crushed and vortexed with ice-cold methanol (10 μl MeOH per mg of tissue) for 15 min at 4°C, the suspension was centrifuged for 1 h at 10,000× g at 4°C, and 50 μl of the supernatant was mixed with 150 μl of 1 M phosphate buffer, pH 2.6. After repeat centrifugation for 15 min at 10,000× g at 4°C, the supernatants were transferred to HPLC vials and analyzed by HPLC with electrochemical detection equipped with a Synergi Polar RP column (Phenomenex; 250 mm × 4.6 mm; 80 Å; 4 μm). All other experimental conditions, the preparation of standards, and analysis of results were as previously described (41).

Statistical analysis. Comparisons of two groups within the same animals (i.e., Left vs. Right arteries) were by paired Student's *t* test, of two groups between different animals (i.e., Ligated vs. Sham operations or 10 vs. 20 wk old) were by unpaired Student's *t* test, and of transcript expression between multiple groups (i.e., Superoxide Inhibition and Vehicle/WT controls) were by one-way analysis of variance using Prism (GraphPad Software). Differences with two-tailed P values < 0.05 were considered to indicate statistical significance.

Online supplemental material. Fig. S1 shows additional morphometric data of common carotid artery remodeling after outflow reduction. Fig. S2 shows histological analyses of medial remodeling. Fig. S3 excludes further potential confounding factors for the differences in vessel phenotypes. Fig. S4

shows flow-mediated vascular remodeling in mice deficient for MyD88-dependent TLR or IL-1 signaling and HPLC analysis for DHE levels in carotid arteries of WT and MyD88$^{-/-}$ mice. Fig. S5 shows transient adventitial T cell and dendritic cell infiltrates and transmural VCAM-1 expression during flow-mediated inward vascular remodeling. Online supplemental material is available at http://www.jem.org/cgi/content/full/jem.20081298/DC1.

We thank Balaraman Kalyanaraman for supporting the superoxide detection experiments.

This work was supported by the National Institutes of Health (NIH; PO1 HL70295). P.C.Y. Tang was supported by a Vascular Research Postdoctoral Training Grant from the NIH (T32 HL07950).

No conflicts of interest exist.

Submitted: 16 June 2008
Accepted: 5 November 2008

REFERENCES

1. Langille, B.L. 1996. Arterial remodeling: relation to hemodynamics. *Can. J. Physiol. Pharmacol.* 74:834–841.
2. Korshunov, V.A., S.M. Schwartz, and B.C. Berk. 2007. Vascular remodeling: hemodynamic and biochemical mechanisms underlying Glagov's phenomenon. *Arterioscler. Thromb. Vasc. Biol.* 27:1722–1728.
3. Kamiya, A., and T. Togawa. 1980. Adaptive regulation of wall shear stress to flow change in the canine carotid artery. *Am. J. Physiol.* 239:H14–H21.
4. Langille, B.L., M.P. Bendeck, and F.W. Keeley. 1989. Adaptations of carotid arteries of young and mature rabbits to reduced carotid blood flow. *Am. J. Physiol.* 256:H931–H939.
5. le Noble, F., D. Moyon, L. Pardanaud, L. Yuan, V. Djonov, R. Matthijsen, C. Bréant, V. Fleury, and A. Eichmann. 2004. Flow regulates arterial-venous differentiation in the chick embryo yolk sac. *Development.* 131:361–375.
6. Hong, H., S. Aksenov, X. Guan, J.T. Fallon, D. Waters, and C. Chen. 2002. Remodeling of small intramyocardial coronary arteries distal to a severe epicardial coronary artery stenosis. *Arterioscler. Thromb. Vasc. Biol.* 22:2059–2065.
7. Mills, I., J.T. Fallon, D. Wrenn, H. Sasken, W. Gray, J. Bier, D. Levine, S. Berman, M. Gilson, and H. Gewirtz. 1994. Adaptive responses of coronary circulation and myocardium to chronic reduction in perfusion pressure and flow. *Am. J. Physiol.* 266:H447–H457.
8. Langille, B.L., and F. O'Donnell. 1986. Reductions in arterial diameter produced by chronic decreases in blood flow are endothelium-dependent. *Science.* 231:405–407.
9. Chatzizisis, Y.S., A.U. Coskun, M. Jonas, E.R. Edelman, C.L. Feldman, and P.H. Stone. 2007. Role of endothelial shear stress in the natural history of coronary atherosclerosis and vascular remodeling: molecular, cellular, and vascular behavior. *J. Am. Coll. Cardiol.* 49:2379–2393.
10. Ungvari, Z., M.S. Wolin, and A. Csiszar. 2006. Mechanosensitive production of reactive oxygen species in endothelial and smooth muscle cells: role in microvascular remodeling? *Antioxid. Redox Signal.* 8:1121–1129.
11. Mohazzab, K.M., P.M. Kaminski, and M.S. Wolin. 1994. NADH oxidoreductase is a major source of superoxide anion in bovine coronary artery endothelium. *Am. J. Physiol.* 266:H2568–H2572.
12. Quintero, M., S.L. Colombo, A. Godfrey, and S. Moncada. 2006. Mitochondria as signaling organelles in the vascular endothelium. *Proc. Natl. Acad. Sci. USA.* 103:5379–5384.
13. Lee, S.B., I.H. Bae, Y.S. Bae, and H.D. Um. 2006. Link between mitochondria and NADPH oxidase 1 isozyme for the sustained production of reactive oxygen species and cell death. *J. Biol. Chem.* 281: 36228–36235.
14. Rajagopalan, S., X.P. Meng, S. Ramasamy, D.G. Harrison, and Z.S. Galis. 1996. Reactive oxygen species produced by macrophage-derived foam cells regulate the activity of vascular matrix metalloproteinases in vitro. Implications for atherosclerotic plaque stability. *J. Clin. Invest.* 98:2572–2579.
15. Castier, Y., R.P. Brandes, G. Leseche, A. Tedgui, and S. Lehoux. 2005. p47phox-dependent NADPH oxidase regulates flow-induced vascular remodeling. *Circ. Res.* 97:533–540.
16. Liu, Y., H. Zhao, H. Li, B. Kalyanaraman, A.C. Nicolosi, and D.D. Gutterman. 2003. Mitochondrial sources of H2O2 generation play a key role in flow-mediated dilation in human coronary resistance arteries. *Circ. Res.* 93:573–580.
17. Mohan, S., N. Mohan, and E.A. Sprague. 1997. Differential activation of NF-kappa B in human aortic endothelial cells conditioned to specific flow environments. *Am. J. Physiol.* 273:C572–C578.
18. Mohan, S., K. Koyoma, A. Thangasamy, H. Nakano, R.D. Glickman, and N. Mohan. 2007. Low shear stress preferentially enhances IKK activity through selective sources of ROS for persistent activation of NF-kappaB in endothelial cells. *Am. J. Physiol. Cell Physiol.* 292: C362–C371.
19. Peters, K., R.E. Unger, J. Brunner, and C.J. Kirkpatrick. 2003. Molecular basis of endothelial dysfunction in sepsis. *Cardiovasc. Res.* 60:49–57.
20. Azevedo, L.C., M. Janiszewski, F.G. Soriano, and F.R. Laurindo. 2006. Redox mechanisms of vascular cell dysfunction in sepsis. *Endocr. Metab. Immune Disord. Drug Targets.* 6:159–164.
21. Rao, D.A., K.J. Tracey, and J.S. Pober. 2007. IL-1alpha and IL-1beta are endogenous mediators linking cell injury to the adaptive alloimmune response. *J. Immunol.* 179:6536–6546.
22. Medzhitov, R., P. Preston-Hurlburt, E. Kopp, A. Stadlen, C. Chen, S. Ghosh, and C.A. Janeway Jr. 1998. MyD88 is an adaptor protein in the hToll/IL-1 receptor family signaling pathways. *Mol. Cell.* 2:253–258.
23. Yamamoto, M., S. Sato, H. Hemmi, K. Hoshino, T. Kaisho, H. Sanjo, O. Takeuchi, M. Sugiyama, M. Okabe, K. Takeda, and S. Akira. 2003. Role of adaptor TRIF in the MyD88-independent toll-like receptor signaling pathway. *Science.* 301:640–643.
24. Sun, D., and A. Ding. 2006. MyD88-mediated stabilization of interferon-gamma-induced cytokine and chemokine mRNA. *Nat. Immunol.* 7:375–381.
25. Hansson, G.K., and P. Libby. 2006. The immune response in atherosclerosis: a double-edged sword. *Nat. Rev. Immunol.* 6:508–519.
26. Hollestelle, S.C., M.R. De Vries, J.K. Van Keulen, A.H. Schoneveld, A. Vink, C.F. Strijder, B.J. Van Middelaar, G. Pasterkamp, P.H. Quax, and D.P. De Kleijn. 2004. Toll-like receptor 4 is involved in outward arterial remodeling. *Circulation.* 109:393–398.
27. Korshunov, V.A., and B.C. Berk. 2004. Strain-dependent vascular remodeling: the "Glagov phenomenon" is genetically determined. *Circulation.* 110:220–226.
28. Walpola, P.L., A.I. Gotlieb, and B.L. Langille. 1993. Monocyte adhesion and changes in endothelial cell number, morphology, and F-actin distribution elicited by low shear stress in vivo. *Am. J. Pathol.* 142:1392–1400.
29. Walpola, P.L., A.I. Gotlieb, M.I. Cybulsky, and B.L. Langille. 1995. Expression of ICAM-1 and VCAM-1 and monocyte adherence in arteries exposed to altered shear stress. *Arterioscler. Thromb. Vasc. Biol.* 15:2–10.
30. Korshunov, V.A., and B.C. Berk. 2003. Flow-induced vascular remodeling in the mouse: a model for carotid intima-media thickening. *Arterioscler. Thromb. Vasc. Biol.* 23:2185–2191.
31. Korshunov, V.A., T.A. Nikonenko, V.A. Tkachuk, A. Brooks, and B.C. Berk. 2006. Interleukin-18 and macrophage migration inhibitory factor are associated with increased carotid intima-media thickening. *Arterioscler. Thromb. Vasc. Biol.* 26:295–300.
32. Kumar, A., J.L. Hoover, C.A. Simmons, V. Lindner, and R.J. Shebuski. 1997. Remodeling and neointimal formation in the carotid artery of normal and P-selectin-deficient mice. *Circulation.* 96:4333–4342.
33. Lessner, S.M., D.E. Martinson, and Z.S. Galis. 2004. Compensatory vascular remodeling during atherosclerotic lesion growth depends on matrix metalloproteinase-9 activity. *Arterioscler. Thromb. Vasc. Biol.* 24:2123–2129.
34. Bakker, E.N., H.L. Matlung, P. Bonta, C.J. de Vries, N. van Rooijen, and E. Vanbavel. 2008. Blood flow-dependent arterial remodelling is facilitated by inflammation but directed by vascular tone. *Cardiovasc. Res.* 78:341–348.

35. Rudic, R.D., E.G. Shesely, N. Maeda, O. Smithies, S.S. Segal, and W.C. Sessa. 1998. Direct evidence for the importance of endothelium-derived nitric oxide in vascular remodeling. *J. Clin. Invest.* 101:731–736.
36. Li, Q., M.M. Harraz, W. Zhou, L.N. Zhang, W. Ding, Y. Zhang, T. Eggleston, C. Yeaman, B. Banfi, and J.F. Engelhardt. 2006. Nox2 and Rac1 regulate H2O2-dependent recruitment of TRAF6 to endosomal interleukin-1 receptor complexes. *Mol. Cell. Biol.* 26:140–154.
37. Dikalov, S., K.K. Griendling, and D.G. Harrison. 2007. Measurement of reactive oxygen species in cardiovascular studies. *Hypertension.* 49:717–727.
38. Rudic, R.D., M. Bucci, D. Fulton, S.S. Segal, and W.C. Sessa. 2000. Temporal events underlying arterial remodeling after chronic flow reduction in mice: correlation of structural changes with a deficit in basal nitric oxide synthesis. *Circ. Res.* 86:1160–1166.
39. Yu, J., S. Bergaya, T. Murata, I.F. Alp, M.P. Bauer, M.I. Lin, M. Drab, T.V. Kurzchalia, R.V. Stan, and W.C. Sessa. 2006. Direct evidence for the role of caveolin-1 and caveolae in mechanotransduction and remodeling of blood vessels. *J. Clin. Invest.* 116:1284–1291.
40. Lei, L., D. Liu, Y. Huang, I. Jovin, S.Y. Shai, T. Kyriakides, R.S. Ross, and F.J. Giordano. 2008. Endothelial expression of beta1 integrin is required for embryonic vascular patterning and postnatal vascular remodeling. *Mol. Cell. Biol.* 28:794–802.
41. Zielonka, J., J. Vasquez-Vivar, and B. Kalyanaraman. 2008. Detection of 2-hydroxyethidium in cellular systems: a unique marker product of superoxide and hydroethidine. *Nat. Protocols.* 3:8–21.
42. McNally, J.S., M.E. Davis, D.P. Giddens, A. Saha, J. Hwang, S. Dikalov, H. Jo, and D.G. Harrison. 2003. Role of xanthine oxidoreductase and NAD(P)H oxidase in endothelial superoxide production in response to oscillatory shear stress. *Am. J. Physiol. Heart Circ. Physiol.* 285:H2290–H2297.
43. Weber, C., W. Erl, A. Pietsch, M. Ströbel, H.W. Ziegler-Heitbrock, and P.C. Weber. 1994. Antioxidants inhibit monocyte adhesion by suppressing nuclear factor-kappa B mobilization and induction of vascular cell adhesion molecule-1 in endothelial cells stimulated to generate radicals. *Arterioscler. Thromb.* 14:1665–1673.
44. Hwang, J., A. Saha, Y.C. Boo, G.P. Sorescu, J.S. McNally, S.M. Holland, S. Dikalov, D.P. Giddens, K.K. Griendling, D.G. Harrison, and H. Jo. 2003. Oscillatory shear stress stimulates endothelial production of O2- from p47phox-dependent NAD(P)H oxidases, leading to monocyte adhesion. *J. Biol. Chem.* 278:47291–47298.
45. Soong, G., B. Reddy, S. Sokol, R. Adamo, and A. Prince. 2004. TLR2 is mobilized into an apical lipid raft receptor complex to signal infection in airway epithelial cells. *J. Clin. Invest.* 113:1482–1489.
46. Into, T., M. Inomata, M. Nakashima, K. Shibata, H. Häcker, and K. Matsushita. 2008. Regulation of MyD88-dependent signaling events by S nitrosylation retards toll-like receptor signal transduction and initiation of acute-phase immune responses. *Mol. Cell. Biol.* 28:1338–1347.
47. Yamamoto, K., T. Sokabe, T. Matsumoto, K. Yoshimura, M. Shibata, N. Ohura, T. Fukuda, T. Sato, K. Sekine, S. Kato, et al. 2006. Impaired flow-dependent control of vascular tone and remodeling in P2X4-deficient mice. *Nat. Med.* 12:133–137.
48. Tzima, E., M. Irani-Tehrani, W.B. Kiosses, E. Dejana, D.A. Schultz, B. Engelhardt, G. Cao, H. DeLisser, and M.A. Schwartz. 2005. A mechanosensory complex that mediates the endothelial cell response to fluid shear stress. *Nature.* 437:426–431.
49. Serbina, N.V., W. Kuziel, R. Flavell, S. Akira, B. Rollins, and E.G. Pamer. 2003. Sequential MyD88-independent and -dependent activation of innate immune responses to intracellular bacterial infection. *Immunity.* 19:891–901.
50. Bolz, D.D., R.S. Sundsbak, Y. Ma, S. Akira, C.J. Kirschning, J.F. Zachary, J.H. Weis, and J.J. Weis. 2004. MyD88 plays a unique role in host defense but not arthritis development in Lyme disease. *J. Immunol.* 173:2003–2010.
51. Liu, N., R.R. Montgomery, S.W. Barthold, and L.K. Bockenstedt. 2004. Myeloid differentiation antigen 88 deficiency impairs pathogen clearance but does not alter inflammation in *Borrelia burgdorferi*-infected mice. *Infect. Immun.* 72:3195–3203.
52. De Ciuceis, C., F. Amiri, P. Brassard, D.H. Endemann, R.M. Touyz, and E.L. Schiffrin. 2005. Reduced vascular remodeling, endothelial dysfunction, and oxidative stress in resistance arteries of angiotensin II-infused macrophage colony-stimulating factor-deficient mice: evidence for a role in inflammation in angiotensin-induced vascular injury. *Arterioscler. Thromb. Vasc. Biol.* 25:2106–2113.
53. Ko, E.A., F. Amiri, N.R. Pandey, D. Javeshghani, E. Leibovitz, R.M. Touyz, and E.L. Schiffrin. 2007. Resistance artery remodeling in deoxycorticosterone acetate-salt hypertension is dependent on vascular inflammation: evidence from m-CSF-deficient mice. *Am. J. Physiol. Heart Circ. Physiol.* 292:H1789–H1795.
54. Bakker, E.N., A. Pistea, J.A. Spaan, T. Rolf, C.J. de Vries, N. van Rooijen, E. Candi, and E. VanBavel. 2006. Flow-dependent remodeling of small arteries in mice deficient for tissue-type transglutaminase: possible compensation by macrophage-derived factor XIII. *Circ. Res.* 99:86–92.
55. Zhang, H., Y. Luo, W. Zhang, Y. He, S. Dai, R. Zhang, Y. Huang, P. Bernatchez, F.J. Giordano, G. Shadel, et al. 2007. Endothelial-specific expression of mitochondrial thioredoxin improves endothelial cell function and reduces atherosclerotic lesions. *Am. J. Pathol.* 170:1108–1120.
56. Benayoun, L., A. Druilhe, M.C. Dombret, M. Aubier, and M. Pretolani. 2003. Airway structural alterations selectively associated with severe asthma. *Am. J. Respir. Crit. Care Med.* 167:1360–1368.
57. Louis, H., A. Kakou, V. Regnault, C. Labat, A. Bressenot, J. Gao-Li, H. Gardner, S.N. Thornton, P. Challande, Z. Li, and P. Lacolley. 2007. Role of alpha1beta1-integrin in arterial stiffness and angiotensin-induced arterial wall hypertrophy in mice. *Am. J. Physiol. Heart Circ. Physiol.* 293:H2597–H2604.
58. Van Rooijen, N., and A. Sanders. 1994. Liposome mediated depletion of macrophages: mechanism of action, preparation of liposomes and applications. *J. Immunol. Methods.* 174:83–93.